

# Spin conservation in high harmonic generation

Emilio Pisanty<sup>1,\*</sup> and Misha Ivanov<sup>1,2,3†</sup>

<sup>1</sup>Blackett Laboratory, Imperial College London, South Kensington Campus, SW7 2AZ London, United Kingdom

<sup>2</sup>Department of Physics, Humboldt University, Newtonstrasse 15, 12489 Berlin, Germany

<sup>3</sup>Max Born Institute, Max Born Strasse 2a, 12489 Berlin, Germany

(Dated: March 10, 2022)

We present an alternative theoretical model for a recent experiment [A. Fleischer *et al.*, arXiv: 1310.1206] which used bichromatic, counter-rotating high intensity laser pulses to probe the conservation of spin angular momentum in high harmonic generation. We separate elliptical polarizations into independent circular fields with definite angular momentum, instead of using the expectation value of spin for each photon in the conservation equation, and we find good agreement with the experimental results. In our description the generation of each individual harmonic conserves spin angular momentum, in contrast to the model proposed by Fleischer *et al.* Our model also correctly describes analogous processes in standard perturbative optics.

The process of high harmonic generation [1] is the flagship experiment of extreme nonlinear optics. It consists of irradiating atoms or small molecules with long-wavelength laser pulses whose electric field is comparable to the internal atomic fields, which results in the emission of harmonics of the driving laser field which can span several thousands of orders [2], most frequently with a flat plateau in their intensity. It can be understood intuitively in terms of a three-step model where an electron is tunnel ionized, propagates classically in the laser field away from the ion and back, and recombines with the ion upon recollision, emitting a burst of high-frequency radiation.

In the final recombination step, the electron rejoins the ion by re-filling the electronic hole it originally left behind, which leaves the ion in its ground state. Thus, although it is usually accompanied by ionization and other processes, high harmonic generation (HHG) is typically seen as a parametric process which leaves the nonlinear medium in its original state. As a parametric process, it must obey conservation laws for energy, momentum, and orbital angular momentum, and these have been successfully demonstrated in the laboratory [3–5].

A recent, ingeniously conceived experiment [6], probes whether the process conserves spin angular momentum. In this experiment, argon atoms are subjected to a superposition of two counter-rotating laser fields of different frequencies [7–10]. This permits the use of driving lasers with spin whilst avoiding the fact that classical trajectories in a single-color circularly-polarized field will miss the ion and thus fail to produce harmonics. In this setup harmonics are produced with nearly the same intensity as for linear fields, with the additional control of the harmonics' polarization through changes in the ellipticity of the driving field.

Fleischer *et al.* [6] have provided a simple model based on perturbative optics which explains the essentials of the spectra they observe, and which shows that the harmonic generation process as a whole does indeed in many cases conserve the spin angular momentum of light. However, they argue that some situations require the electron to carry away angular momentum after the recollision.

Their model, which we refer to as Model 1 hereafter, suggests that spin angular momentum is not conserved for

certain harmonic lines, so that some harmonics must be assumed to be emitted in correlated pairs for the overall process to be parametric. Additionally, an “extreme nonlinear optics correction term” is introduced by hand, and for certain harmonics the model’s predictions depend discontinuously on the experimental parameters in a way we find unphysical.

In this paper we present an alternative perturbative-optics model for this experiment. In essence, we posit that, as regards nonlinear optics, elliptically polarized fields should be seen as the superposition of circularly polarized fields of different amplitudes which contribute photons of definite spin  $\sigma = \pm 1$ , instead of single photons that contribute their expected spin  $|\sigma| < 1$ . This model accounts for the same experimental results as Model 1 without any free parameters, and it does not have unphysical discontinuities. Further, it provides specific predictions that can be tested numerically (and, in principle, experimentally), by shifting the relative frequency of the two circular components of elliptical light. Within this model, the generation of each harmonic is a closed process that does conserve spin angular momentum.

This paper is structured as follows. In §I we review the essentials of the experiment and Model 1. In §II we present our own model, Model 2, and explain its differences to Model 1. In §III we describe a four-wave mixing process that embodies, within the domain of perturbative optics, the differences between the two models.

## I. THE EXPERIMENT

The experiment of Fleischer *et al.* [6] uses two copropagating equal-intensity laser drivers. One is centred at 800 nm and the other, at 410 nm, is obtained from the longer wavelength by a red-shifted second harmonic generation setup; the slightly-off-integer ratio between the frequencies helps identify how many photons from each field have been absorbed. Both linearly-polarized drivers go through quarter-wave plates which are free to rotate independently, and the drivers are then combined.

The resulting electric field performs a variety of Lissajous figures in the polarization plane, which slowly drift throughout the pulse due to the slight anharmonicity between the drivers. The pulses comprise about fourteen cycles of the fundamental and thus equally many passes of the Lissajous figure. In the symmetric setting, with both pulses

\* e.pisanty11@imperial.ac.uk

† m.ivanov@imperial.ac.uk

circularly polarized, the Lissajous figure is a trifolium. The harmonic spectrum in this case covers the integer orders not divisible by three.

The experimental observations consist of two scans over the ellipticity of each of the drivers while the other is held constant at the circular polarization. This opens up a variety of subsidiary channels, including channels at orders divisible by 3, which are otherwise forbidden by parity. These subsidiary channels are slightly detuned from the main ones, which is due to the slightly off-integer ratio  $r = 1.95$  between the frequencies of the two drivers. This detuning enables a unique assignment of integers  $n_1$  and  $n_2$  of photons absorbed from each driver, in terms of which the frequency of each channel is

$$\Omega_{(n_1, n_2)} = n_1\omega + n_2r\omega, \quad (1)$$

where  $n_1 + n_2$  must be odd by conservation of parity.

In Model 1, each driver is considered to contribute a spin  $\sigma_j$  per photon to the process, where  $\sigma_j$ ,  $j = 1, 2$ , is the expectation value of angular momentum corresponding to the polarization state of driver  $j$ . In the symmetric setting, the fundamental driver's polarization is right circular, with complex unit vector  $\hat{\mathbf{e}}_R = \frac{1}{\sqrt{2}}(\hat{\mathbf{e}}_H + i\hat{\mathbf{e}}_V)$ , and its photons have definite spin  $\sigma_1 = +1$ . Similarly, the harmonic driver is left-circular polarized along  $\hat{\mathbf{e}}_L$ , and its photons have definite spin  $\sigma_2 = -1$ .

In the general case each driver is elliptically polarized and can be written in the form

$$\mathbf{E} = \frac{E_0 e^{-i\omega t}}{2\sqrt{2}} \left( \frac{1+\varepsilon}{\sqrt{1+\varepsilon^2}} \hat{\mathbf{e}}_R + \frac{1-\varepsilon}{\sqrt{1+\varepsilon^2}} \hat{\mathbf{e}}_L \right) + \text{c.c.}, \quad (2)$$

where  $\varepsilon \in [-1, 1]$  is the signed ellipticity of the field. The expected angular momentum of this field can be calculated to be

$$\langle \hat{\sigma} \rangle = \frac{2\varepsilon}{1+\varepsilon^2} \quad (3)$$

in units of  $\hbar$ . For a field generated by shining linearly polarized light on a half-wave plate at an angle  $\alpha$  to its fast axis, as in the experiment, this reduces to  $\langle \hat{\sigma} \rangle = \sin(2\alpha)$ .

The main assumption of the model, that each photon contributes its expected angular momentum to the process, can now be expressed formally. The spin of the resulting harmonic photon on the channel  $(n_1, n_2)$  must be

$$\sigma_{(n_1, n_2)} = n_1\sigma_1 + n_2\sigma_2 + \delta_{(n_1, n_2)}, \quad (4)$$

where  $\sigma_1 = \langle \hat{\sigma}_1 \rangle = \sin(2\alpha)$  and  $\sigma_2 = \langle \hat{\sigma}_2 \rangle = \sin(2\beta)$ , and  $\alpha$  and  $\beta$  are the angles of the fast axes of the waveplates to the initial linear polarization.

Here each of the three angular momenta can be measured independently, both experimentally and numerically, so that a deviation term  $\delta_{(n_1, n_2)}$  has been introduced for consistency. Within Model 1, the harmonic generation process is parametric if and only if this term is zero. Fleischer *et al.* attribute deviations from this to the failure of perturbative nonlinear optics, and call  $\delta_{(n_1, n_2)}$  an “extreme nonlinear optics correction term”. Model 1 makes multiple predictions which agree with the experiment, though some of them require nonzero values of  $\delta_{(n_1, n_2)}$ .

1. For the symmetric case that  $\alpha = \beta = 45^\circ$ , so  $\sigma_1 = 1$  and  $\sigma_2 = -1$ , setting  $\delta_{(n_1, n_2)} = 0$  turns the basic relation (4) into  $\sigma_{(n_1, n_2)} = n_1 - n_2$ . From here, imposing the boundedness of photon spins,  $|\sigma_{(n_1, n_2)}| \leq 1$ , coupled with the parity constraint, means that  $n_1$  and  $n_2$  must differ by unity, which matches the experimental predictions.

2. As the fundamental driver's waveplate is rotated away from the symmetric case, this restriction must be expanded to include the magnitude of  $\sigma_2$ , and now reads

$$|n_1 \sin(2\alpha) - n_2| \leq 1. \quad (5)$$

For each channel  $n_1$  and  $n_2$  are fixed, so this reads as a restriction on  $\alpha$ , and gives the region where the channel is allowed:

$$\frac{1}{2} \arcsin\left(\frac{n_2 - 1}{n_1}\right) \leq \alpha \leq \frac{1}{2} \arcsin\left(\frac{n_2 + 1}{n_1}\right). \quad (6)$$

This region matches well the observed range of the channels (7,6), (8,7), and (9,8). For the channels (13,4), (12,5), (11,6), (10,7) and (9,8), this restriction also correctly predicts a V-shaped pattern where decreasing harmonic order gives an allowed region further from  $\alpha = 45^\circ$ . On the other hand, to actually get the correct regions, correction factors as high as  $|\delta_{(n_1, n_2)}| = 3$  are required, and these are not consistent across these channels.

3. For certain channels like (6,7) or (7,8), the restriction (5) gives a region of the form

$$\sin(2\alpha) \geq 1 \quad (7)$$

when  $\delta_{(n_1, n_2)}$  is set to zero. If one insists on the harmonic generation process being parametric, these channels are only allowed for  $\alpha = 45^\circ$ , but not for any infinitesimally different angle. This discontinuity is not present elsewhere in the formalism, and it is not observed in experiment or in simulations, so one is forced, within Model 1, to abandon conservation of spin angular momentum in the generation each individual harmonic.

4. In its form  $\frac{n_2 - 1}{n_1} \leq \sin(2\alpha)$ , the restriction (5) means that, for  $\beta$  fixed at  $45^\circ$ , only channels with  $n_1 \geq n_2 - 1$  can exist, which is in agreement with experiment.

Finally, within this model it is possible to study the deviation  $\delta_{(n_1, n_2)}$  as a function of the experimental parameters. It is shown in Ref. 6 that the average of this quantity over all the channels tends to be close to zero, which is argued to be indicative of angular momentum transfers between different harmonics, or even the possibility that harmonics are emitted in pairs, with the production of each pair conserving angular momentum. This is indeed possible, in principle, and in such a process Eq. (4) would be replaced by a more general conservation law for the two correlated channels seen as a single process.

## II. DECOMPOSITION-BASED MODEL

We now present an alternative model for this experiment, which explains the above features while still allowing for the generation of each harmonic to preserve spin angular momentum independently of the other channels. The key to this model is seeing Eq. (2) as indicating the presence of a third wave which must be included as such, instead of a change to the angular momentum carried by each photon of the driver.

To bring this to the forefront, we rephrase Eq. (2) in the form

$$\mathbf{E} = \frac{E_0 e^{-i\omega t}}{2} (\cos(\delta\alpha) \hat{\mathbf{e}}_R + \sin(\delta\alpha) \hat{\mathbf{e}}_L) + \text{c.c.}, \quad (8)$$

where  $\delta\alpha = \alpha - \pi/4$  and we have used  $\varepsilon = \tan(\alpha)$ . We focus for simplicity on the case where  $\beta$  is fixed at  $45^\circ$ .

Within Model 2, the problem consists now of *three* waves which can combine to form harmonics: a left-circular harmonic driver at frequency  $r\omega = 1.95\omega$ , and two fundamental drivers at frequency  $\omega$ , one right-circular with relative amplitude  $\cos(\delta\alpha)$ , and one left-circular with relative amplitude  $\sin(\delta\alpha)$ . Each channel is now characterized by three integers,  $(n_+, n_-, n_2)$ , where  $n_+$  ( $n_-$ ) photons are absorbed from the right- (left-)circular fundamental driver, and  $n_2$  from the harmonic driver, to give an emitted frequency of

$$\Omega_{(n_+, n_-, n_2)} = (n_+ + n_-)\omega + n_2 r\omega. \quad (9)$$

Certain channels require negative values for  $n_-$  or  $n_+$  for one or both spins of the harmonic photon. In this case, the channel represents stimulated emission into that driver. This is necessary, for example, to explain the generation of elliptically polarized photons on channels of the form  $(n_1, n_1 + 1)$  like  $(6, 7)$  and  $(7, 8)$ .

Each field has photons of a definite spin, which means that the conservation of angular momentum reads in this model as

$$\sigma_{(n_+, n_-, n_2)} = n_+ \sigma_+ + n_- \sigma_- + n_2 \sigma_2, \quad (10)$$

where  $\sigma_+ = +1$  and  $\sigma_- = \sigma_2 = -1$ .

To obtain predictions, we apply the basic principle that the amplitude of an  $n$ -photon process should scale as the  $n^{\text{th}}$  power of the driving field, which is the generalization to nonlinear optics of Einstein's  $B$  coefficient formalism. This applies both to absorption and to stimulated emission.

As the waveplate is rotated away from the symmetric setting at  $\alpha = 45^\circ$ , the initial energy is transferred from the right-circular driver to the left-circular one. Each channel  $(n_+, n_-, n_2)$  absorbs an independent number of photons from each driver, which means that its amplitude must have a basic dependence of the form

$$E_{(n_+, n_-, n_2)} \sim \cos^{|n_+|}(\delta\alpha) \sin^{|n_-|}(\delta\alpha); \quad (11)$$

the harmonic intensity is the square of this. For most channels  $n_+$  and  $n_-$  are relatively large integers, so the functions in Eq. (11) can be rather sharply peaked. Within this model there are no hard boundaries to the existence regions, and the harmonics are in principle possible for any set of laser parameters. Instead, the predictions are in terms for the basic profile of each channel as a function of the driver ellipticity.

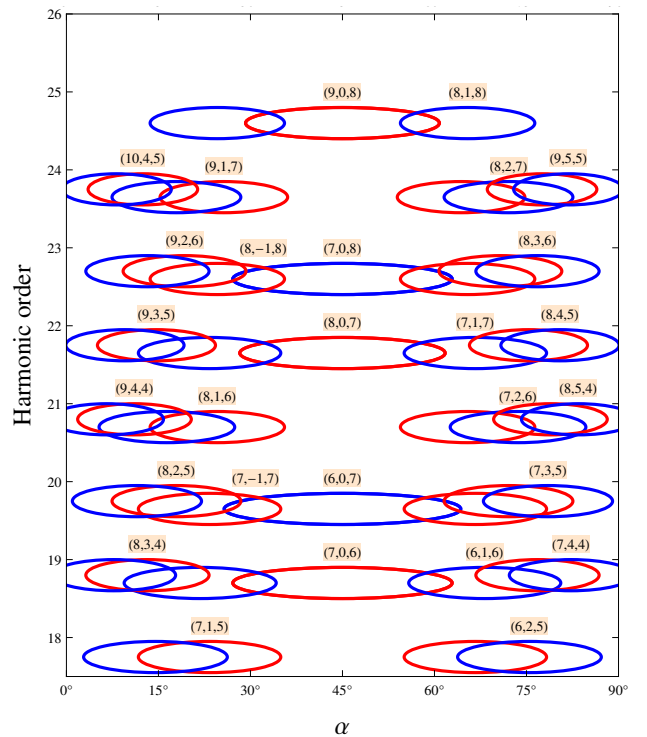


FIG. 1. Existence regions for the different harmonics predicted by Model 2 presented as ellipses. The red ellipses, with labels on the left, have spin  $+1$ , while the blue ellipses, with labels on the right, have spin  $-1$ . The ellipses are drawn, with arbitrary widths, at half-maximum intensity as predicted by Eq. (11).

A good approximation to where each channel is relevant is the region where it is above half of its maximum intensity; we display these regions in Fig. 1. One interesting feature of this model is that each channel splits into two different channels with opposite spin. For example, the channel identified as  $(10,5)$  in Model 1, at frequency  $\Omega = (10 + 5r)\omega$ , splits into the two channels  $(8,2,5)$  and  $(7,3,5)$ , with spin  $+1$  and  $-1$  respectively. In general, the channel  $(n_1, n_2)$  splits into the channels

$$(n_+, n_-, n_2) = \left( \frac{n_1 + n_2 + \sigma}{2}, \frac{n_1 - n_2 - \sigma}{2}, n_2 \right) \quad (12)$$

with spin  $\sigma = \pm 1$ . For this expression to give integer  $n_\pm$ ,  $n_1 + n_2$  must be an odd integer, which matches the parity constraint of Model 1.

As is seen in Fig. 1, the existence regions for these two channels overlap but do not coincide, and they agree rather well with the numerical results of Ref. 6 without any free parameters. The superposition of right- and left-circular contributions whose amplitude peaks at different driver ellipticities helps explain the rich dynamics of the polarization of each harmonic shown by experiment. On the other hand, certain predicted channels appear not to contribute in the entire regions or to only do so weakly, when compared with numerics [6].

One particularly important feature of this model is its behaviour for channels of the form  $(n_1, 0, n_1 + 1)$ , like  $(6,0,7)$ . As remarked in point 3 above, conservation of angular momentum closes this channel for  $\alpha \neq 45^\circ$ , because the harmonic driver contributes  $-7$  units of angular momentum, and this can only be offset by the  $6\sin(2\alpha)$  units of the

fundamental driver when  $\sin(2\alpha) = 1$ . Within Model 2, a slightly off-circular field can still produce harmonics: it is seen as a circular field of slightly reduced intensity, with the added presence of a left-circular driver which cannot participate in the process at that order, and must do so through the stimulated-emission channel (7, -1, 7).

The other predictions of Model 1 can also be replicated. The symmetric case is identical for both models, so the restriction that  $|n_1 + n_2| = 1$  there also holds; the V-shaped pattern is explained well together with the existence regions of the harmonics; and the restriction that  $n_1 \geq n_2 - 1$  is a consequence of the identity  $n_+ = n_- + n_2 + \sigma$ .

In addition to this, Model 2 can make specific predictions of its own. In particular, and similarly to the way that the different channels are tagged in Ref. [6] by a slight detuning in one of the drivers, one can in principle tag the two circular components of the fundamental driver, as in Eq. (8), with different frequencies. This can be tested both experimentally and numerically and should have the effect of spectrally splitting the two components of each channel; if the correct shifts are detected it would confirm this model as the correct one.

### III. A FOUR-WAVE MIXING ANALOG

Having reviewed both models, we now present a perturbative-optics treatment of a case analogous to the channels of the form  $(n_1, 0, n_1+1)$ , where conservation of angular momentum is hardest to reconcile with Model 1. We rephrase Model 2 in this setting and we show that it coincides with the predictions of standard, perturbative, nonlinear optics.

In particular, consider a four-wave mixing set-up where two intense drivers of different frequencies,  $\omega_1$  and  $\omega_2$ , are directed at a gas jet or a fibre with an isotropic third-order susceptibility tensor  $\overset{\leftrightarrow}{\chi}^{(3)}$  to generate a harmonic field at frequency  $\omega_3 = 2\omega_1 + \omega_2$  [11], as shown in Fig. 2. Suppose, additionally, that the driver at  $\omega_1$  is fixed at a left circular polarization, while the ellipticity  $\varepsilon$  of the  $\omega_2$  driver can be varied from right circular through linear to left circular.

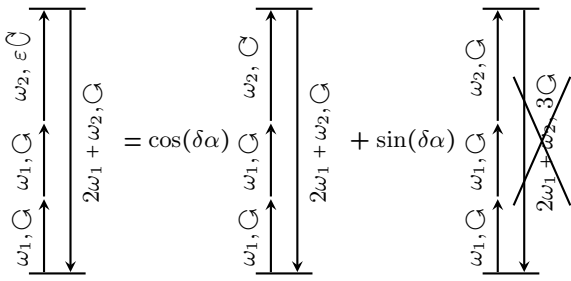


FIG. 2. Four-wave mixing scheme where an intense left-circular driver at frequency  $\omega_1$  and an elliptically polarized driver at frequency  $\omega_2$  produce a left-circular harmonic at frequency  $2\omega_1 + \omega_2$ . By decomposing the elliptical driver as a superposition of circular polarizations, as in Eqs. (2) and (8), one obtains an allowed process with a right-circular  $\omega_2$  driver, and a forbidden process with three left-circular drivers which has too much angular momentum for a single  $2\omega_1 + \omega_2$  photon.

From the perspective of Model 1, the process cannot happen unless the  $\omega_2$  driver has a right circular polarization, with an ellipticity of  $\varepsilon = 1$ . If the field is even slightly elliptical, the expectation value of the second driver's spin per photon decreases to  $\sigma = 2\varepsilon/(1+\varepsilon^2) = \sin(2\alpha) < 1$ , and there is no longer a way for the total spin to be bounded by 1.

Within Model 2, on the other hand, the elliptical driver is understood as a superposition of circular drivers of spin  $\pm 1$  with amplitude  $(1 \pm \varepsilon)/\sqrt{2(1 + \varepsilon^2)}$ . If the polarization is slightly off-circular, most of the amplitude is in the right-circular driver, which can still participate in the process, and a slightly reduced harmonic is obtained.

More specifically, as the allowed process takes in one photon from the right-circular component at frequency  $\omega_2$ , the harmonic field will be proportional to the component's amplitude,

$$E \sim \frac{1 + \varepsilon}{\sqrt{2(1 + \varepsilon^2)}} = \cos(\delta\alpha),$$

where  $\alpha = \frac{\pi}{4} + \delta\alpha$  is the corresponding waveplate setting. The output intensity will be the square of this. Note, in particular, that there will be some nonzero harmonic intensity for *all* ellipticities except for the completely left-circular case, which includes many cases with negative expectation value of the photon spin.

The predictions of Model 2 are in complete agreement with the predictions of standard perturbative nonlinear optics [12, 13], which was shown early on to conserve spin angular momentum [14, 15]. In this treatment, the sum-frequency wave at  $\omega_3 = 2\omega_1 + \omega_2$  is generated by the nonlinear polarization

$$\mathbf{P}^{(3)} = \epsilon_0 \overset{\leftrightarrow}{\chi}^{(3)} : \mathbf{E} \mathbf{E} \mathbf{E}, \quad (13)$$

where the vertical dots denote a three-way tensor contraction. In component form, this relation reads  $P_i^{(3)} = \epsilon_0 \sum_{jkl} \overset{\leftrightarrow}{\chi}^{(3)}_{ijkl} E_j E_k E_l$ .

To obtain the sum-frequency component of this polarization, one expresses the electric field as a sum over the participating modes,

$$\mathbf{E} = \sum_{\alpha=1}^3 \left[ \mathbf{E}_\alpha e^{i(\mathbf{k}_\alpha \cdot \mathbf{r} - \omega_\alpha t)} + \mathbf{E}_\alpha^* e^{-i(\mathbf{k}_\alpha \cdot \mathbf{r} - \omega_\alpha t)} \right] \quad (14)$$

and looks for the component of the polarization which oscillates as  $e^{i(\mathbf{k}_3 \cdot \mathbf{r} - \omega_3 t)}$ . Substituting the expression (14) into the contraction in (13) results in eight terms, depending on whether  $\mathbf{E}_\alpha$  or its conjugate is taken. Each of the eight terms describes a different process, which include parametric amplification or self- and cross-phase modulation [13]; the sum-frequency generation process we want is the term with three factors of  $\mathbf{E}_\alpha$ , with the polarization amplitude

$$\mathbf{P}_4 = \epsilon_0 \overset{\leftrightarrow}{\chi}^{(3)} : \mathbf{E}_1 \mathbf{E}_1 \mathbf{E}_2 e^{i\varphi}, \quad (15)$$

where  $\varphi = (2\mathbf{k}_1 + \mathbf{k}_2 - \mathbf{k}_3) \cdot \mathbf{r} - (2\omega_1 + \omega_2 - \omega_3)t$ .

To calculate the contraction in Eq. (15) we impose the isotropy condition on the susceptibility tensor  $\overset{\leftrightarrow}{\chi}^{(3)}$ . The only isotropic tensors of rank 4 have a component form  $\delta_{ij}\delta_{kl}$  [16, §3.03], which corresponds to the tensor action

$$\overset{\leftrightarrow}{\delta} : \mathbf{uvw} = \mathbf{u}(\mathbf{v} \cdot \mathbf{w}).$$

That is, the tensor contracts its second and third inputs, and produces a vector along its first input. The contraction in (15) produces three terms of this form, with different

permutations of its inputs. Each of these terms will in principle have a different frequency-dependent complex scalar susceptibility  $\chi_s^{(3)}(\omega_\alpha, \omega_\beta, \omega_\gamma)$ , but only one term will be allowed so this distinction can be dropped.

Under these conditions, the sum-frequency polarization becomes

$$\mathbf{P}_4 = \epsilon_0 \chi_s^{(3)} e^{i\varphi} \left( 2\mathbf{E}_1(\mathbf{E}_1 \cdot \mathbf{E}_2) + \mathbf{E}_2(\mathbf{E}_1 \cdot \mathbf{E}_1) \right). \quad (16)$$

Here  $\mathbf{E}_1 = E_1 \hat{\mathbf{e}}_L$  is left polarized, which means that the second term vanishes: in a frame where the propagation direction is in the  $z$  axis,

$$\hat{\mathbf{e}}_L \cdot \hat{\mathbf{e}}_L = \frac{1}{\sqrt{2}} \begin{pmatrix} 1 \\ i \\ 0 \end{pmatrix} \cdot \frac{1}{\sqrt{2}} \begin{pmatrix} 1 \\ i \\ 0 \end{pmatrix} = 0. \quad (17)$$

The amplitude for the field at  $\omega_2$  encodes the ellipticity dependence, through the analog of Eq. (2),

$$\mathbf{E}_2 = E_2 \left( \frac{1+\varepsilon}{\sqrt{2(1+\varepsilon^2)}} \hat{\mathbf{e}}_R + \frac{1-\varepsilon}{\sqrt{2(1+\varepsilon^2)}} \hat{\mathbf{e}}_L \right). \quad (18)$$

This is projected on the amplitude  $\mathbf{E}_1$ , and multiplies the left-circular vector  $\mathbf{E}_1$ , so that the final amplitude is

$$\mathbf{P}_4 = \epsilon_0 \chi_s^{(3)} e^{i\varphi} E_1^2 E_2 \frac{1+\varepsilon}{\sqrt{2(1+\varepsilon^2)}} \hat{\mathbf{e}}_L. \quad (19)$$

The ellipticity dependence of this result is exactly that predicted by Model 2, whereas Model 1 predicts the process is forbidden except for  $\varepsilon = 1$ . In perturbative optics, then using the expectation value of each photon's angular momentum in the conservation equation leads to incorrect results. This is fundamentally due to the fact that perturbative optics is, in a sense, more multilinear than it is nonlinear.

It is beneficial and important to try to provide an intuitive understanding of extreme nonlinear phenomena like HHG in terms of a simple photon picture. It is indeed conceivable that in situations where many different diagrams contribute to the response the final output will be well approximated by a nonlinear function of single-photon expectation values. However, even in such a setting one must ensure that each individual diagram being counted is indeed allowed, and that the model that uses such diagrams stands a test in the perturbative regime.

For the particular experiment of Ref. [6], then, spin angular momentum is seen to be conserved for the generation of each individual harmonic, at least as far as perturbative optical models are applicable.

We gratefully acknowledge fruitful discussions with A. Fleischer and O. Cohen, who made their results available prior to publication. This work was funded by EPSRC Program Grant EP/I032517/1 and the CORINF Training Network. E. P. gratefully acknowledges support from CONACYT.

---

[1] M. IVANOV AND O. SMIRNOVA. Multielectron High Harmonic Generation: simple man on a complex plane. In T. SCHULTZ AND M. VRAKKING (eds.), *Attosecond and Free Electron Laser science*, chap. 1, pp. 1–55 (2013). arXiv:1304.2413 [physics.atom-ph]; C. JOACHAIN, M. DÖRR AND N. KYLSTRA. High-intensity laser-atom physics. *Adv. At., Mol., Opt. Phys.* **42** (2000), pp. 225–286. ULB e-print.

[2] T. POPMINTCHEV, M.-C. CHEN, D. POPMINTCHEV et al. Bright coherent ultrahigh harmonics in the kev x-ray regime from mid-infrared femtosecond lasers. *Science* **336** no. 6086 (2012), pp. 1287–1291. JILA e-print.

[3] M. D. PERRY AND J. K. CRANE. High-order harmonic emission from mixed fields. *Phys. Rev. A* **48** no. 6 (1993), pp. R4051–R4054.

[4] J. B. BERTRAND, H. J. WÖRNER, H.-C. BANDULET, É. BISSON, M. SPANNER, J.-C. KIEFFER, D. M. VILLENEUVE AND P. B. CORKUM. Ultrahigh-order wave mixing in noncollinear high harmonic generation. *Phys. Rev. Lett.* **106** no. 2 (2011), p. 023 001.

[5] M. ZÜRCH, C. KERN, P. HANSINGER, A. DREISCHUH AND C. SPIELMANN. Strong-field physics with singular light beams. *Nature Phys.* **8** no. 10 (2012), pp. 743–746.

[6] A. FLEISCHER, O. KFIR, T. DISKIN, P. SIDORENKO AND O. COHEN. Does High Harmonic Generation conserve angular momentum?. *Nature Photon.* Accepted, arXiv:1310.1206 [physics.optics].

[7] D. B. MILOŠEVIĆ AND B. PIRAX. High-order harmonic generation in a bichromatic elliptically polarized laser field. *Phys. Rev. A* **54** no. 2 (1996), pp. 1522–1531.

[8] D. B. MILOŠEVIĆ, W. BECKER AND R. KOPOLD. Generation of circularly polarized high-order harmonics by two-color coplanar field mixing. *Phys. Rev. A* **61** no. 6 (2000), p. 063 403.

[9] F. CECCHERINI, D. BAUER AND F. CORNOLTI. Harmonic generation by atoms in circularly polarized two-color laser fields with coplanar polarizations and commensurate frequencies. *Phys. Rev. A* **68** no. 5 (2003), p. 053 402. arXiv: physics/0211110 [physics.atom-ph].

[10] D. B. MILOŠEVIĆ AND W. BECKER. Attosecond pulse generation by bicircular fields: from pulse trains to a single pulse. *Journal of Modern Optics* **52** no. 2–3 (2005), pp. 233–241.

[11] H. J. SIMON AND N. BLOEMBERGEN. Second-harmonic light generation in crystals with natural optical activity. *Phys. Rev.* **171** no. 3 (1968), pp. 1104–1114.

[12] Q. LIN AND G. P. AGRAWAL. Vector theory of four-wave mixing: polarization effects in fiber-optic parametric amplifiers. *J. Opt. Soc. Am. B* **21** no. 6 (2004), pp. 1216–1224.

[13] G. P. AGRAWAL. *Nonlinear Fiber Optics* (Academic Press, Boston, 1989).

[14] N. BLOEMBERGEN. Conservation laws in nonlinear optics. *J. Opt. Soc. Am.* **70** no. 12 (1980), p. 1429.

[15] C. L. TANG AND H. RABIN. Selection rules for circularly polarized waves in nonlinear optics. *Phys. Rev. B* **3** no. 12 (1971), pp. 4025–4034.

[16] H. JEFFREYS AND B. S. JEFFREYS. *Methods of Mathematical Physics*. 3 ed. (Cambridge University Press, 1965). arXiv:13960/t3hx2br67.